Deploying a Continuous Wave Electromagnetic Disturbance Removal Algorithm on an OFDM System

Aleksandr Ovechkin
ESAT-WaveCore, M-Group
KU Leuven, Bruges Campus
B-8200 Brugge, Belgium
aleksandr.ovechkin@kuleuven.be

Brian Leeman
ESAT-WaveCore, M-Group
KU Leuven, Bruges Campus
B-8200 Brugge, Belgium
brian.leeman@kuleuven.be

Dries Vanoost
ESAT-WaveCore, M-Group
KU Leuven, Bruges Campus
B-8200 Brugge, Belgium
dries.vanoost@kuleuven.be

Tim Claeys
ESAT-WaveCore, M-Group
KU Leuven, Bruges Campus
B-8200 Brugge, Belgium
tim.claeys@kuleuven.be

Guy A. E. Vandenbosch
ESAT-WaveCore
KU Leuven
3001 Leuven, Belgium
guy.vandenbosch@kuleuven.be

Davy Pissoort
ESAT-WaveCore, M-Group
KU Leuven, Bruges Campus
B-8200 Brugge, Belgium
davy.pissoort@kuleuven.be

***Abstract*—This paper describes the physical validation of the continuous wave electromagnetic disturbance removal algorithm for orthogonal frequency division multiplexing communication systems. The validation is done by deploying the algorithm in a laboratory setting. Due to the assumptions being made during the simulation process of the algorithm, the validation process describes the key aspects that must be taken into account during actual deployment. For instance, it is shown that in orthogonal frequency division multiplexing-based systems, a continuous wave disturbance can completely break equalization. Therefore, to perform validation, the disturbance has to be injected so that it will not affect the signal's preamble. During the validation, it was shown that the algorithm under investigation is effective and can result in the algorithm's gain of more than 18 dB for specific bit error rate ratios and modulation schemes.**

***Index Terms*—Orthogonal frequency division multiplexing (OFDM), electromagnetic disturbance (EMD), narrowband interference (NBI), noise cancellation, continuous wave (CW)**

I. Introduction

Nowadays, the world is going towards complete "digitalization". This creates a valid demand for increased data speed communication, signal coverage and dependability. The latter term can relate to multiple aspects. However, this work focuses on dependability in terms of data communication safety and robustness in different communication environments. This is a valid concern, especially in systems for safety-critical systems. Autonomous systems (ASs) represent a cluster of safety-critical systems.

The ASs have to comply with very stringent requirements. As a result, reliability for some use cases should be at least 99.999 % and the maximum latency should not exceed 3 ms [1]. High reliability and low latency mean a message must be delivered in one go and understood correctly. The ASs must also remain reliable in diverse environments, including the electromagnetic (EM) environment. However, it is shown that orthogonal frequency division multiplexing (OFDM), which is an underlying wireless communication technology of ASs [2], is susceptible to narrowband interferences (NBIs). These interferences can be represented as continuous wave (CW) electromagnetic disturbances (EMDs). OFDM systems are susceptible to a spectral leakage phenomenon, which makes ASs vulnerable to CW EMDs [3], [4]. This means that a potential vulnerability to CW EMDs must be tackled before the mass deployment of ASs.

Suppose we insert a CW EMD exactly on a subcarrier. In that case, the CW EMD will only disturb this subcarrier. However, any other misalignment of a CW EMD concerning subcarriers leads to spectral leakage to multiple subcarriers due to non-coherent sampling. This can be solved by implementing coding or interleaving techniques, or their combination [5], [6].

Different research groups have investigated the spectral leakage problem. Their solutions can be categorized into those that primarily rely on frequency-domain [7], time-domain [8], or both time- and frequency-domain [9] techniques. In this paper, the chosen CW EMD removal algorithm is a frequency-domain solution based on the spectral leakage property [6]. The proposed mathematical model [6] calculates a mismatch between the carrier and CW frequencies by demodulating and modulating the received OFDM signal again. Based on the frequency mismatch between the carrier and CW EMD frequencies, two main CW parameters (amplitude and phase) are identified. The CW EMD is reconstructed and subtracted from the noisy signal with these estimated parameters.

The research leading to these results has received funding from the European Union's Horizon 2020 research and innovation programme under the Marie Skłodowska-Curie Grant Agreement No 812.788 (MSCA-ETN SAS).

This publication reflects only the authors' view, exempting the European Union from any liability. Project website: http://etn-sas.eu/.

979-8-3503-2400-6/23/$31.00 ©2023 IEEE

This paper takes the CW EMD removal algorithm's mathematical model and deploys it in an OFDM system in a laboratory setting. The IEEE 802.11a [10] standard forms the basis for the OFDM system. Therefore, the algorithm [6] is adapted during the deployment procedure. After that, a series of measurements with different CW EMD configurations is performed.

The remainder of this paper is organized as follows: Section II provides the CW EMD removal algorithm's mathematical model which is vital for the following analysis. Section III pinpoints the issues that were faced during the deployment process. It also provides the adaptations with the used OFDM system and the algorithm that had to be taken for validation purposes. Section IV provides the measurement results and analysis by comparing these results with the recreated simulations. The final thoughts and conclusions are presented in Section V.

II. Fundamentals of the CW EMD removal algorithm

To better understand the algorithm under validation, let us provide the key points of the CW EMD removal algorithm. A more in-depth explanation can be found in [6]. A simplified version of the CW EMD removal algorithm is presented in Fig. 1. Let us navigate through it.

After performing the needed data transformations (FFT, parallel-to-serial conversion and equalization), the captured OFDM sequence R_m (m - is a subcarrier number) undergoes the demodulation and re-modulation processes that result in data estimations S^*_m. The "*" sign is introduced since it is unknown in advance whether the estimation is erroneous or not. The error estimation E^*_m is obtained by taking the difference between the result after the de- and re-modulation processes S^*_m and the received initial R_m sequence. Ideally, if there was no EMD or any other noise in the system, the de- and re-modulation processes would result in data coinciding with R_m. With a CW EMD present, the obtained data can still be correctly demodulated (if the CW EMD is not large enough to induce a symbol flip). However, this paper focuses on cases when a CW EMD introduces a symbol flip on one or more subcarriers. This means that the de- and re-modulation processes substitute a symbol with the erroneous one. This erroneous symbol further results in the erroneous E^*_m estimation. However, this happens when the CW EMD is large enough. The error estimations E^*_m are used for calculating the frequency mismatch between the CW and carrier frequencies f_{diff}:

$$f_{\text{diff}} = \frac{jBd}{2\pi} ln\left(\frac{E^*_m - E^*_{m+\frac{K}{2}}}{E^*_m + E^*_{m+\frac{K}{2}}} e^{j2\pi m/K}\right), \quad (1)$$

where Bd is the baud rate and K is the total number of subcarriers which is an even number.

Equation (1) shows that f_{diff} is derived by taking a ratio between a difference and the sum of two halves of the error vector E^*_m. As a result, f_{diff} will only have $K/2$ values. In ideal conditions, the f_{diff} values are real numbers. However, this is seldom the case due to numerical precision, external noise signals comprising the system's noise and erroneous E^*_m estimations. The five f_{diff} values with the lowest imaginary part are selected to reach the best result. From these values, the median is chosen as the best estimation for f_{diff}. The remaining CW parameters, such as amplitude and phase, are calculated as a complex amplitude:

$$A_{\text{CW}} e^{-j\theta_{\text{CW}}} = \left(\frac{E^*_m + E^*_{m+\frac{K}{2}}}{\sum_{n=0}^{K-1}\left(e^{-j2\pi n(f_{\text{diff}}/Bd + m/K)}(1 - e^{-j\pi n})\right)}\right), \quad (2)$$

where n represents a sample number.

With the known CW parameters, one may reconstruct the EMD using the following equation:

$$E^*_m = A_{\text{CW}} \sum_{n=0}^{K-1}\left(e^{-j(2\pi f_{\text{diff}} n/Bd + \theta_{\text{CW}})} e^{-j2\pi mn/K}\right). \quad (3)$$

Finally, the reconstructed E_m is subtracted from the received OFDM sequence R_m resulting in an improved FFT output.

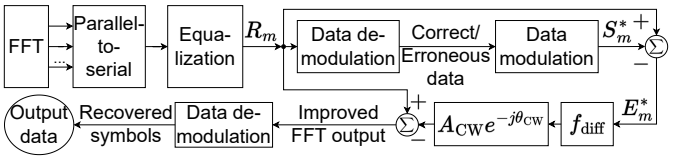

Fig. 1. The CW EMD removal algorithm's block scheme.

III. Algorithm's deployment

The CW EMD removal algorithm [6] was derived assuming that the communication system was both time and frequency synchronized and there were no reflections or multipath fading. Such an assumption is acceptable at the initial stage of conceiving a theory, deriving it mathematically and testing it in simulations. When it comes to testing in lab settings caution must be taken.

A. Equalization issues

The OFDM communication system, recreated in this work, is based on the WLAN 802.11a standard [10]. This means that an OFDM frame consists of a preamble and an OFDM symbol each of which differs in duration and how they are created (the header was omitted since the modulation parameters and the OFDM symbol's length were constant during the tests). The OFDM symbol consists of pilot and data subcarriers.

A preamble consists of training sequences called legacy short and long training fields (LSTF and LLTF, respectively). These training sequences are prepended to an OFDM frame in the time domain and consist of multiple identical sequences. Fig. 2a represents the preamble of an OFDM frame when no disturbance happens. Black dashed lines subdivide the

identical LSTF sequences, while the red lines serve to delimit the parts of LLTF which consist of an extended cyclic prefix and two long sequences, each with a length of an OFDM symbol. When a CW EMD is injected into the channel, the EMD's energy disturbs not only the payload but also the OFDM's preamble. This disrupts the repetitiveness between LSTF and LLTF sequences in the OFDM's preamble. Fig. 2b represents this phenomenon and shows the case when CW EMD happens precisely between two contiguous subcarriers.

Consequently, equalization cannot be done properly since it is based on autocorrelating repeatable preamble's LLTF sequences. As a result, a CW EMD has to be injected into the system while not affecting the preamble. Therefore, it was decided to add the CW EMD in code on a transmitted OFDM frame and let the preamble part of the OFDM signal be CW-free.

B. Synchronizing the validation system

The used transmitter and receiver can be frequency synchronized by using the same local reference frequency of 10 MHz. As for timing synchronization a set of actions called the "Bruteforce" timing synchronization method was used.

Once the receiver captures an incoming signal, the "Bruteforce" timing synchronization method starts working to locate the beginning of an OFDM frame. This search calculates the bit error rate (BER) and signal-to-noise (SNR) for every sample. The sample with the lowest BER and largest SNR is deemed to be the beginning of the OFDM frame. The

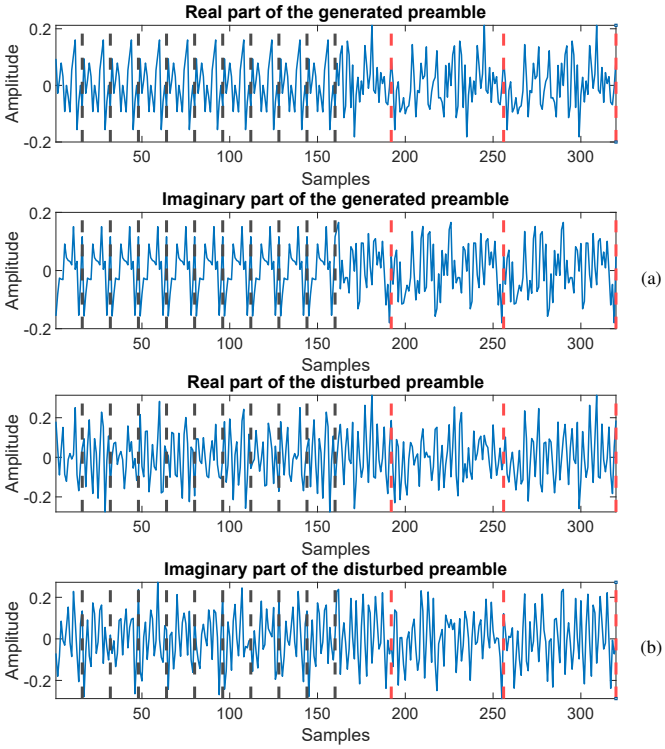

Fig. 2. Real & imaginary values of the OFDM preamble when a CW EMD is not present on the preamble (a), and when it disturbs it (b).

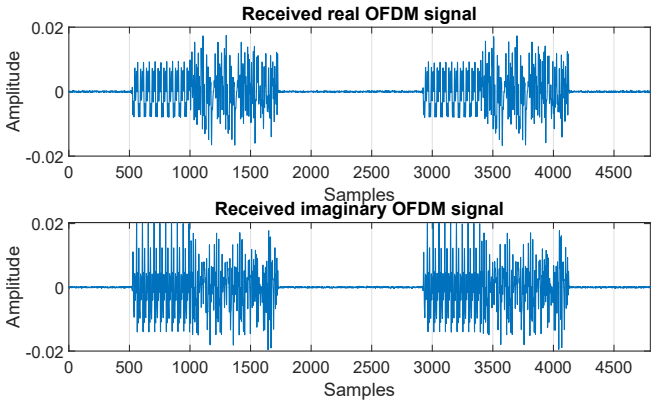

Fig. 3. Real and imaginary received noisy (SIR = 25 dB) values of the transmitted OFDM signal using RS devices.

"Bruteforce" method is easy to realize, however, it makes the validation not real-time, i.e. it cannot immediately start a new communication session before the synchronization ends. Nevertheless, this method allows for identifying the beginning of an OFDM frame and subsequently performing the algorithm, which is the main goal that had to be achieved.

Let us describe the "Bruteforce" method and its work using the real example of the two used devices. The Rohde & Schwarz (RS) SMM100A [11] is a vector signal generator that was used as the transmitter, while the RS FSVA3000 [12] is a signal and spectrum analyzer that was used as the receiver. The devices were frequency synchronized (10 MHz reference frequency) and the system noise was decreased by using a cabled connection between the devices. The OFDM frame's composition was based upon [10], except for the header that was not used in our system. An OFDM signal was created in Matlab [13]. The generated signal contained a full OFDM frame plus an "idle" period in which zeroes were transmitted. The transmitter was constantly sending the same generated sequence, so the "idle" period was done intentionally for better visualization at the receiver's side.

The receiver was set up to obtain at least two OFDM signals. For a better signal resolution and SNR, an oversampling took place. For QAM16 with 64 subcarriers an OFDM frame has a length of 400 samples. With an "idle" period it becomes 800. Considering the receiver's capturing time and an oversampling of three, one can witness in Fig. 3 4800 received samples.

The created OFDM system can be found in Fig. 4 in which a CW EMD is added into the system after the inverse fast Fourier transform and the addition of a cyclic prefix.

The calculated parameters needed for the "Bruteforce" synchronization method are shown in Fig. 5. For defining SNR, the "Bruteforce" method exploits the built-in Matlab function that calculates the modulation error rate (MER). It can be deemed as a form of an SNR measurement since it calculates the average deviation of the received I-Q symbols from the reference constellation points.

Looking back at Fig. 5, one may notice that the number of calculations differs from the number of samples shown

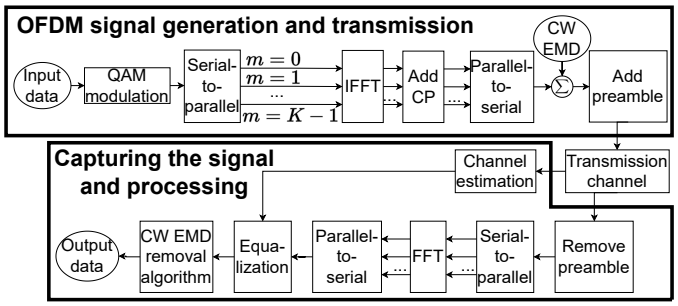

Fig. 4. The created OFDM system for validation.

in Fig. 3. Given that the sample number is 400 and an oversampling factor is 3, the number of calculations will become 3600 (see Fig. 5). Despite the difference, a noticeable correlation is visible between these figures. Analyzing Fig. 5 further, one may notice that the smallest BER (0 %) and the maximum SNR value ($\approx$ 24.9 dB) happen at the 2905$^{\text{th}}$ sample.

IV. Validation measurements

The validation measurements were performed at the KU Leuven, Bruges Campus test facility. First, an OFDM packet and a CW EMD are created on a computer. After that, the noisy packet is sent via the Ethernet cable to the transmitter which is connected via a radio frequency (RF) cable to the receiver. Via this cable, the noisy packet reaches the transmitter. Finally, the captured signal is sent via the Ethernet cable back to the computer. The latter performs the needed processing which consists of the OFDM packet search and the CW EMD removal algorithm implementation.

A. Defining the validation parameters

The main system and CW EMD parameters are outlined in Table I. The modulation scheme was chosen to be QAM16 because, as was shown in [14], the algorithm performs the best with the lowest possible modulation scheme order. For a better analysis, the receiver performed oversampling, meaning that the receiver's sampling frequency was larger than the one of the transmitter. A CW EMD was constructed and injected into the OFDM system so that it will be always exactly between two contiguous subcarriers. In this way, the resulting after the FFT block spectral leakage will have a detrimental effect. Therefore, no extra coding techniques such as Hamming or interleaving were used, in contrast to [6].

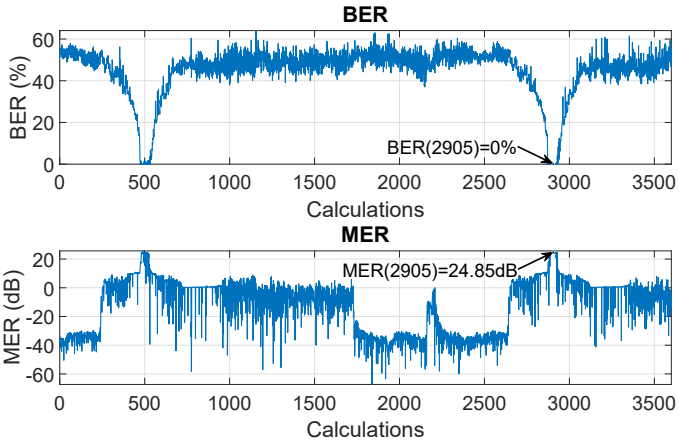

Fig. 5. BER and MER of the received noisy (SIR = 25 dB) OFDM signal.

TABLE I
OFDM and CW EMD parameters

Parameter	Value
Modulation scheme	QPSK, QAM16, QAM64
Number of subcarriers, K	64
Direct current (DC) subcarrier	Yes
Pilot subcarriers	[12, 26, 40, 54]
Guardband subcarriers	6 on the left and 5 on the right
Baud rate, Bd	100
Clock rate, MHz	100
Signal power, dBm	-30
Oversampling factor at the receiver's side	3
Subcarrier width, H	Bd/K
CW EMD phase (θ_{CW}), degree	45
Distance to the closest CW EMD subcarrier, α	0.5
SIR span[a], dB	[-50:25]
SIR step, dB	5
CW EMD amplitude, A_{CW}	$A_{\text{CW}} = \frac{S_{\text{RMS}}}{10^{\text{SIR}/20}}$

[a] During the measurements, per every SIR value, five bit sequences were used to result in a smoother result after averaging.

Let us characterize the spectral leakage by the spectral leakage parameter α that will be equal to a relative distance of a CW EMD between two subcarriers. In our case, α is equal to 0.5.

The SIR for a CW EMD was calculated as:

$$\text{SIR} = 20\log_{10}(\frac{S_{\text{RMS}}}{A_{\text{CW}}}), \tag{4}$$

where S_{RMS} is the root mean square value of the signal, while A_{CW} denotes the amplitude of the interference.

B. Hardware limitations

One aspect of real communication often excluded in simulations is the receiver's ability to regulate the power of the incoming signal. This regulation is called automatic gain control (AGC). AGC makes the output power stay constant in order to ensure the maximum resolution of the analog-to-digital converter. This means that low-power signals are amplified and vice-versa.

Let us look at Fig. 6, which shows the system's BER response to a varying CW EMD that does not create spectral leakage ($\alpha = 0$). The BER response is measured when the algorithm is deactivated. The results are shown for both simulations and physical measurements. The simulation results are shown with a blue dashed line. It can be noticed that starting from an SIR level of 10 dB, the BER performance of the system does not change anymore with a decrease in the SIR level. However, this is not the case for measurements (look at the black solid line). While perfectly coinciding with the simulations curve until the SIR value of -25 dB, the measurements' BER results start degrading at SIR values lower than -25 dB. This happens due to the aforementioned AGC. After the AGC, the OFDM signal becomes so small that it reaches the noise level of the AGC. This means that the quantization noise on the OFDM signal is largely increased. It leads to data loss resulting in BER degradation.

Since the scope of this paper is to validate the algorithm under a broad SIR span, the data loss at low SIR levels due to AGC puts hardware limitations on the algorithm. This means that the algorithm can be validated up to a specific SIR.

C. Measurement results

Before measurements with a CW EMD, white noise was measured. It was equal to 35.3 dB. The BER of the OFDM system under validation with a CW EMD inserted in the OFDM symbol is shown in Fig. 7. The dashed blue line presents the algorithm's performance, while the solid black line is the reference performance of the system without the algorithm. It can be seen that both curves have almost no bit errors at SIR levels higher than 20 dB. Both the reference and algorithm curves gradually increase their BER value with the decrease in SIR values, with the reference curve increasing its BER values earlier. Therefore, a visible difference between the two curves can be seen. For better visualization, a magnified part can also be seen in Fig. 7. With this magnified part, it is easier to estimate the algorithm's gain (a difference in dB between the reference and algorithm curves for a given BER level) for the BER levels between 1 and 10 %. For example, for the BER level of 1 %, the algorithm's gain is 5.9 dB, while

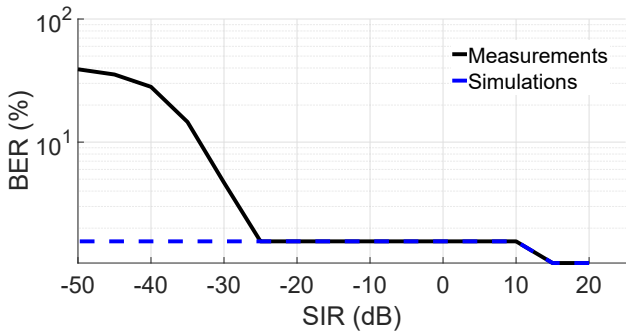

Fig. 6. The BER performance of the system when there is no spectral leakage ($\alpha = 0$), $\theta_{CW} = 45°$.

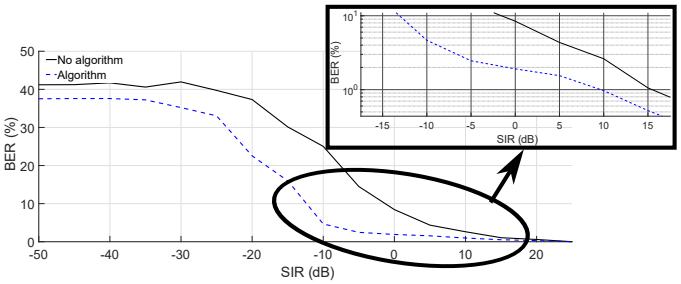

Fig. 7. The BER performance of the system when the spectral leakage parameter $\alpha = 0.5$.

for other BER levels, it increases and reaches its maximum value of $\approx$ 15.1 dB for the BER level of 3 %.

The algorithm's gain for other BER levels up to 5 % is calculated and presented in Fig. 8. This figure also shows the gain for QPSK and QAM64 modulation schemes used in OFDM, which complies with [10]. For QPSK, the maximum gain is 18.36 dB for a BER level of 3 %, while for QAM64 it is equal to 11.05 dB for a BER level of 4 %. This shift in the maximum algorithm's gain (the highest and lowest are for QPSK and QAM64, respectively) can be explained by a change in the OFDM itself. The lower the modulation order scheme is used, the more robust the system is. As has already been investigated in [14], the system benefits from the algorithm the most at low modulation order schemes. Also, once the maximum gain for a particular modulation scheme at a certain BER level has been reached, the algorithm's gain decreases. As shown in Fig. 6, this happens due to a rising disturbance power and AGC, after which a digitization error occurs and the algorithm makes wrong estimations.

The presented measurement results in Figs. 7 and 8 cannot be compared with previous simulations presented in [6] as "A-to-B" for a few reasons. First, simulations do not account for the work of AGC. Second, guardband and DC subcarriers were not used in the simulations. During the validation procedure, these subcarriers carried no information and as a result, were unmodulated. This means that these subcarriers could be directly used for defining the spectral leakage pattern of a CW EMD. Because of no re-modulation procedure on these subcarriers, the chance of the wrong CW EMD estimation is minimal. The same can be applied to pilot subcarriers that also

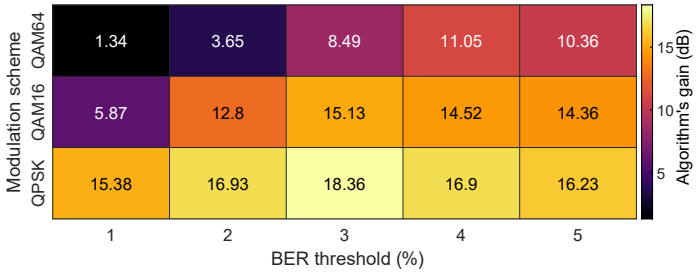

Fig. 8. The algorithm's gain for different modulation schemes when the spectral leakage parameter $\alpha = 0.5$.

do not undergo the re-modulation procedure since the pilot values are known. Nevertheless, the presented measurements show that the algorithm succeeds in removing a CW EMD since the BER performance of the OFDM system improves.

V. Conclusion

The CW EMD removal algorithm for OFDM-based systems described in [6] was practically validated in this paper. The algorithm was tested for QPSK, QAM16 and QAM64 based upon [10]. The initial measurement tests showed that equalization does not work correctly if a CW EMD is injected into the transmitted OFDM signal. A CW EMD makes the preamble parts too different to perform a proper autocorrelation. Therefore, the CW EMD was injected in code so that only OFDM symbols were disturbed, meaning the preamble was unaffected by the generated CW. This allowed performing correct equalization. The used devices were frequency synchronized by using the same local reference frequency. The timing synchronization was done by capturing an OFDM sequence and performing BER and SNR measurements on the obtained signal. The sample with the lowest BER and largest SNR value was used as the frame's beginning.

During the validation measurements, it was shown that irrespective of the algorithm's performance, the BER performance of the system will decrease as the SIR level becomes lower. This happens due to hardware limitations caused by the receiver's built-in AGC that could not be considered in simulations. In addition, the algorithm's realization and the environments in which it was tested differed in the originally published algorithm and the system under validation. This means an "A-to-B" comparison between the simulation and validation results cannot occur. Nevertheless, the algorithm's gain during the validation measurements reached ≈ 18.4 dB at the BER level of 3 % for the QPSK modulation scheme.

The validation results showed that the algorithm is deployable on real equipment in laboratory settings with certain hardware and software adjustments. The algorithm works and the system benefits from it. However, further research has to be performed regarding synchronization and algorithm compatibility to be able to deploy the algorithm on a real-time OFDM system.

References

[1] G. Naik, B. Choudhury, and J.-M. Park, "IEEE 802.11bd & 5G NR V2X: Evolution of Radio Access Technologies for V2X Communications," *IEEE Access*, vol. 7, pp. 70 169–70 184, 2019.

[2] A. Ovechkin, "Future Wireless Communication Protocols in Autonomous Systems," available at: https://etn-sas.eu/2020/03/23/future-wireless-communication-protocols-in-autonomous-systems/, accessed: May 2, 2023.

[3] K. M. Fors, K. C. Wiklundh, and P. F. Stenumgaard, "On the Mismatch of Emission Requirements for CW Interference Against OFDM Systems," *IEEE Transactions on Electromagnetic Compatibility*, vol. 60, no. 5, pp. 1555–1561, Oct 2018.

[4] K. Fors, E. Axell, S. Linder, and P. Stenumgaard, "On the Impact of CW interference on 5G NR," *EMC Europe 2019 - 2019 International Symposium on Electromagnetic Compatibility*, pp. 1049–1054, 2019.

[5] Y. Shi, X. M. Zhang, Z.-C. Ni, and N. Ansari, "Interleaving for combating bursts of errors," *IEEE Circuits and Systems Magazine*, vol. 4, no. 1, pp. 29–42, 2004.

[6] A. Ovechkin, T. Claeys, D. Vanoost, G. A. E. Vandenbosch, and D. Pissoort, "A Novel Method of Removing the Influence of Continuous Electromagnetic Wave Disturbances in OFDM Systems," *IEEE Transactions on Electromagnetic Compatibility*, pp. 1–10, 2021.

[7] T. Zhao, H. Zhao, Y. Zhao, X. Cheng, and B. Ai, "A Frequency-Domain Estimation Scheme for Single-Tone Interference in OFDM Systems," in *2011 Third International Conference on Communications and Mobile Computing*, 2011, pp. 409–412.

[8] A. Coulson, "Bit error rate performance of OFDM in narrowband interference with excision filtering," *IEEE Transactions on Wireless Communications*, vol. 5, no. 9, pp. 2484–2492, Sep. 2006.

[9] T. Pande, I. H. Kim, and A. Batra, "A method for narrowband interference mitigation in OFDM by minimizing spectral leakage," in *2015 IEEE International Symposium on Power Line Communications and Its Applications (ISPLC)*, March 2015, pp. 19–23.

[10] "IEEE Standard for Information Technology–Telecommunications and Information Exchange between Systems - Local and Metropolitan Area Networks–Specific Requirements - Part 11: Wireless LAN Medium Access Control (MAC) and Physical Layer (PHY) Specifications," *IEEE Std 802.11-2020 (Revision of IEEE Std 802.11-2016)*, pp. 1–4379, 2021.

[11] "R&S©SMM100A vector signal generator."

[12] "R&S©FSVA3000 Signal and spectrum analyzer."

[13] "The MathWorks Inc. MATLAB 9.13.0.2049777 (R2022b)," 2022.

[14] A. Ovechkin, B. Leeman, D. Vanoost, T. Claeys, G. A. E. Vandenbosch, and D. Pissoort, "Influence of AWGN on the Possibility to Remove a Continuous Wave EM Disturbance in OFDM systems," in *2022 International Symposium on Electromagnetic Compatibility – EMC Europe*, 2022, pp. 667–672.